EMBRY-RIDDLE
Aeronautical University™

SCHOLARLY COMMONS

Publications

Spectroscopic and Photometric Analysis of HS 1136+6646: A Hot Young DAO+K7 V Post-Common-Envelope, Pre-Cataclysmic Variable Binary

D. K. Sing
University of Arizona

Terry D. Oswalt
Florida Institute of Technology, oswaltt1@erau.edu

J. B. Holberg
University of Arizona

M. R. Burleigh
University of Leicester

S. A. Good
University of Leicester

See next page for additional authors

Follow this and additional works at: https://commons.erau.edu/publication

Part of the Stars, Interstellar Medium and the Galaxy Commons

Scholarly Commons Citation

Sing, D., Oswalt, T. D., Holberg, J., Burleigh, M., Good, S., & al., e. (2004). Spectroscopic and Photometric Analysis of HS 1136+6646: A Hot Young DAO+K7 V Post-Common-Envelope, Pre-Cataclysmic Variable Binary. *The Astronomical Journal, 127*(5). https://doi.org/10.1086/386354

Authors

D. K. Sing, Terry D. Oswalt, J. B. Holberg, M. R. Burleigh, S. A. Good, and et al.

SPECTROSCOPIC AND PHOTOMETRIC ANALYSIS OF HS 1136+6646: A HOT YOUNG DAO+K7 V POST–COMMON-ENVELOPE, PRE–CATACLYSMIC VARIABLE BINARY[1,2]

D. K. SING,[3,4] J. B. HOLBERG,[3,4] M. R. BURLEIGH,[5] S. A. GOOD,[5] M. A. BARSTOW,[5] T. D. OSWALT,[6] S. B. HOWELL,[7] C. S. BRINKWORTH,[8] M. RUDKIN,[6] K. JOHNSTON,[6] AND S. RAFFERTY[6]

ABSTRACT

Extensive photometric and spectroscopic observations have been obtained for HS 1136+6646. The observations reveal a newly formed post–common-envelope binary system containing a hot $\sim$DAO.5 primary and a highly irradiated secondary. HS 1136+6646 is the most extreme example yet of a class of short-period hot H-rich white dwarfs with K–M companion systems such as V471 Tau and Feige 24. HS 1136+6646 is a double-line spectroscopic binary showing emission lines of H I, He II, C II, Ca II, and Mg II, due in part to irradiation of the K7 V secondary by the hot white dwarf. Echelle spectra reveal the hydrogen emission lines to be double-peaked with widths of $\sim$200 km s^{-1}, raising the possibility that emission from an optically thin disk may also contribute. The emission lines are observed to disappear near the inferior conjunction. An orbital period of 0.83607 ± 0.00003 days has been determined through the phasing of radial velocities, emission-line equivalent widths, and photometric measurements spanning a range of 24 months. Radial velocity measurements yield an amplitude of $K_{\mathrm{WD}} = 69 \pm 2$ km s^{-1} for the white dwarf and $K_{\mathrm{K7V}} = 115 \pm 1$ km s^{-1} for the secondary star. In addition to orbital variations, photometric measurements have also revealed a low-amplitude modulation with a period of 113.13 minutes and a semiamplitude of 0.0093 mag. These short-period modulations are possibly associated with the rotation of the white dwarf. From fits of the Balmer line profiles, the white dwarf is estimated to have an effective temperature and gravity of $\sim$70,000 K and $\log g \sim 7.75$, respectively. However, this optically derived temperature is difficult to reconcile with the far-UV spectrum of the Lyman line region. *Far Ultraviolet Spectroscopic Explorer* spectra show the presence of O VI absorption lines and a spectral energy distribution whose slope persists nearly to the Lyman limit. The extremely high temperature of the white dwarf, from both optical and UV measurements, indicates that the binary system is one of the earliest post–common-envelope objects known, having an age around 7.7×10^5 yr. Although the spectrum of the secondary star is best represented by a K7 V star, indications are that the star may be overly luminous for its mass.

Key words: binaries: spectroscopic — white dwarfs

1. INTRODUCTION

Post–common-envelope binary systems evolve from relatively widely separated main-sequence stars. As both stars mature, the more massive component evolves faster, becoming a red giant or supergiant and overflowing its Roche lobe. The onset of unstable mass transfer then causes the stars to spiral closer together, decreasing their orbital period. As the stars spiral inward and mass is transferred to the less massive star, eventually producing an extended atmosphere, a common envelope (CE) develops around both companions. The two stars then transfer orbital angular momentum to the envelope while they spiral inward, helping to eject its outer layers. The resulting system is a detached binary with the primary star cooling toward the white dwarf stage.

CE evolution is a poorly understood process affecting the evolution of many close binary systems including cataclysmic variables (CVs), Type Ia supernovae, millisecond pulsars, and X-ray binaries with neutron star or black hole components. It is not known exactly how efficiently the red giant's CE is ejected, how much mass is lost in the process, or how much the orbital separation will decrease. Post-CE binaries provide important observational constraints on theoretical models of CE evolution as well as improving our understanding of the evolution, space density, and period distribution of CVs. Only about 25 post-CE binaries have measured orbital periods and far fewer have accurate component masses. Thus, the study of every newly discovered system provides the potential for important new information.

The DAO star HS 1136+6646 (hereafter HS 1136) was first discovered by Heber, Dreizler, & Hagen (1996) during follow-up spectroscopy of stellar sources from the Hamburg-Schmidt objective-prism survey. The authors classified HS 1136 as a binary star consisting of a hot DAO (He II $\lambda 4686$

TABLE 1
HS 1136+6646 System Parameters

Parameter	Value	Note
R.A. (J2000)	$11^h39^m05^s.98$	
Decl. (J2000)...	$+66°30'17''.98$	
V magnitude..	13.63 ± 0.03	
J magnitude...	12.314 ± 0.021	
H magnitude..	11.695 ± 0.024	
K magnitude..	11.543 ± 0.021	
V_{dK}...	15.46 ± 0.04	Inferior conjunction estimate
V_{WD}	13.85 ± 0.03	
V-band photometric semiamplitude (orbital) (mag)	0.11	
V-band photometric semiamplitude (rotational) (mag)	0.0093	
White dwarf DAOT_{eff} (K)...................................	$\approx 70{,}000$	$\log g \sim 7.75$
White dwarf rotational (?) period (minutes)	113.13	
K dwarf spectral type	K4–7 V	
Radial velocity ephemeris T_0....................................	HJD $2452360.566 \pm 0.83607E$	
K_{WD} velocity (km s^{-1})	69 ± 2	
K_{dK} velocity (km s^{-1})	130 ± 7	
γ system (km s^{-1})	-20.9 ± 1	
γ (km s^{-1})...	12.1 ± 5	
M_{dK} ($M_\odot$)	0.34	
M_{WD} ($M_\odot$)	0.63	
a ($R_\odot$)...	3.7 ± 0.1	Orbital separation
Estimated distance (pc)	388^{+100}_{-50}	

in absorption) with a late K companion. No emission lines were seen in the 1993 March 11, 1:14 UT (U. Heber 2004, private communication) spectrum, despite the fact that our ephemeris (see Table 1) places the phase at 0.64 ± 0.1, when the emission lines should be visible. A combination of significantly lower resolution along with all of the strongest emission lines observed between 4000 and 7000 Å falling in the cores of the white dwarf's broad photospheric absorption lines is a possible reason for the lack of visual emission lines. Moreover, the Heber spectra do not extend shortward of 4000 Å, where some of the strongest emission lines are observed.

The coordinates of HS 1136, derived from the STScI Digital Sky Survey plates, are included in Table 1 along with a finding chart in Figure 1. Estimates of proper motion derived from the USNO-B1.0 catalog (Monet et al. 2003) indicate a proper motion of $0''.065$ yr^{-1} at a position angle of $248°$.

We first observed HS 1136 on 2001 March 15 with the Steward Observatory 2.4 m telescope as part of a spectroscopic survey of DAO and H-rich planetary nebula central stars. At that time its spectrum was dramatically different from that published by Heber et al. (1996). Strong emission lines due to H I, He II, Ca II, and Mg II were observed. Follow-up observations on 2001 May 5–6, 2002 March 26–29, and 2003 March 21–23 showed a large-amplitude orbital motion between the emission lines and the He II $\lambda 4686$ photospheric absorption line, due to the white dwarf, as expected in a double-line spectroscopic binary for discussion of these initial observations see Holberg et al. (2001) and Sing et al. (2002).

In this paper we present a complete description of the existing ground-based data including the 2003 observations, refine the system parameters, and present two newly discovered properties of the white dwarf and the secondary star. In §§ 2 and 3 we discuss the spectroscopic and photometric observations that are analyzed in § 4. In § 5 we interpret the

parameters derived for HS 1136 and compare it with similar post-CE systems.

2. SPECTROSCOPIC OBSERVATIONS

2.1. *Bok Spectroscopic Observations*

The radial velocity measurements were obtained on the Steward Observatory 2.4 m Bok telescope, located on Kitt Peak, during three observing runs between 2001 May and 2003 March (see Table 2). The spectra were obtained using the Boller & Chivens Spectrograph at the Ritchey-Chrétien f/9 focus. A 1200×800 15 μm pixel CCD was used in combination with a first-order 1200 line mm^{-1} grating blazed at 5436 Å to record the blue channel spectra covering a wavelength range of 3880–5040 Å. With a $2''.5$ slit width, a typical spectral resolution of 3.5 Å was achieved at a reciprocal dispersion of 0.99 Å pixel^{-1} on the CCD. Typical exposure times of 1000–1200 s yielded characteristic signal-to-noise ratios (S/N) of 50–60. Before each observation, the instrument was rotated to align the slit perpendicular to the horizon, minimizing the effects of atmospheric dispersion.

Standard Image Reduction and Analysis Facility (IRAF) routines were used to reduce the data. The wavelength calibration was established with HeAr arc-lamp spectra, interpolated between exposures taken before and after each observation, to account for any small wavelength shifts that may occur while the telescope tracks an object. The spectra were flux calibrated using the Massey et al. (1988) spectrophotometric standard Feige 34 observed over a range of zenith angles covering the program stars' air-mass range. HR 4550 and HD 103095 were used as radial velocity standards.

Radial velocities of the K7 V companion were extracted from the unresolved emission lines in the optical data by the following procedure using standard IRAF packages. A template image was formed by first flattening all the HS 1136 observations with a thirtieth-order spline to remove the continuum, applying a heliocentric velocity correction for each
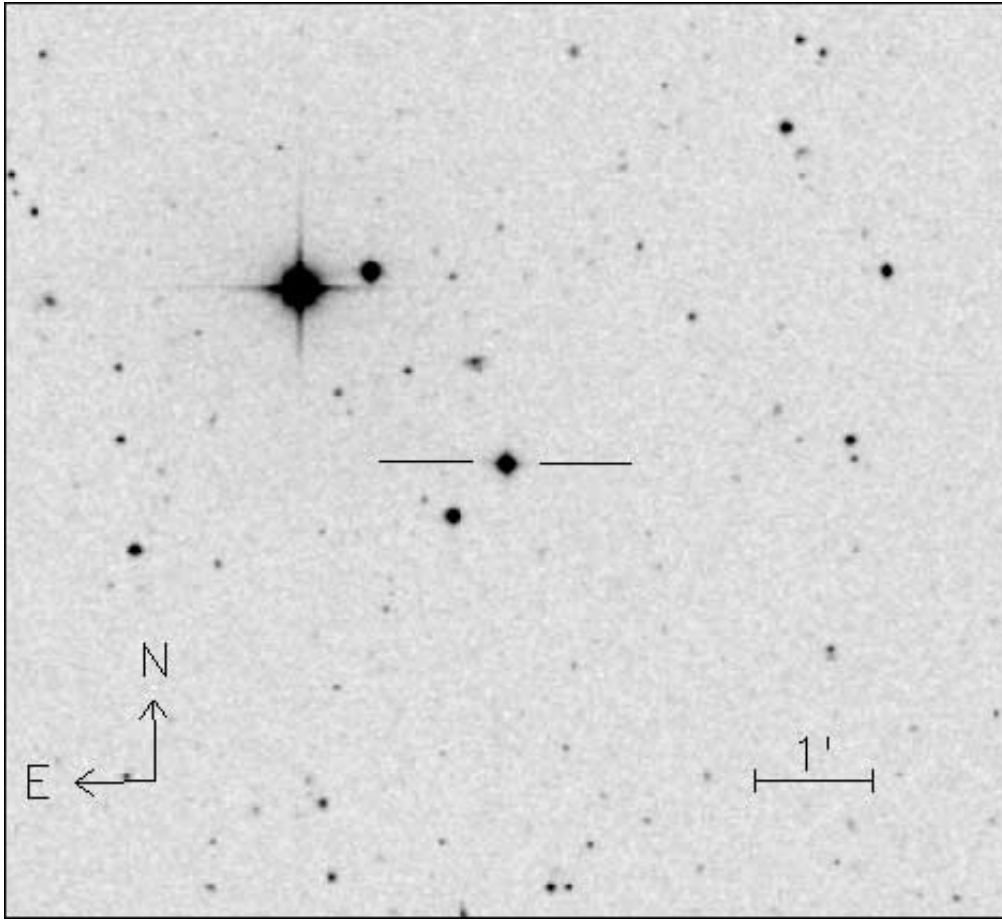
Fig. 1.—Digital Sky Survey finding chart (POSS II, *blue*) for HS 1136+6646

TABLE 2
Log of Spectroscopic Observations

Date	MJD Start (JD − 2,450,000)	MJD End (JD − 2,450,000)	Telescope[a]	Spectral Range[b]	No. Observations
2001 Jan 29............	1921.85486	1921.96217	*FUSE*	FUV	2
2001 Mar 15	1984.91318	1984.92952	Bok	Blue	2[c]
2001 May 05..........	2035.65081	2035.94868	Bok	Blue	18[d]
2001 May 06..........	2036.63678	2036.84621	Bok	Blue	18[d]
2001 Dec. 20	2264.85638	2264.93835	Bok	Blue	5
2001 Dec 21	2265.99446	2266.00834	Bok	Blue	1
2002 Jan 03............	2277.82778	2277.84861	Mayall	Red	1
2002 Jan 04............	2278.83333	2279.01389	Mayall	Red	4
2002 Jan 29............	2303.64792	2303.73803	*FUSE*	FUV	2
2002 Mar 26	2360.63557	2360.99945	Bok	Blue	14[c]
2002 Mar 27	2361.65752	2361.98831	Bok	Blue	14[c]
2002 Mar 28	2362.69017	2362.98201	Bok	Blue	11[c]
2002 Mar 29	2363.62567	2363.96778	Bok	Blue	18[c]
2002 Dec 18	2627.80817	2628.05427	Bok	Red	13[c]
2003 Mar 21	2720.62975	2721.01248	Bok	Blue	16[c]
2003 Mar 22	2721.61615	2722.00100	Bok	Blue	18[c]
2003 Mar 23	2722.63475	2723.00905	Bok	Blue	19[c]
2003 May 14..........	2773.31983	2774.93389	*FUSE*	FUV	18

[a] (Bok) Steward Observatory 2.3 m telescope at Kitt Peak; (Mayall) NOAO 4 m telescope at Kitt Peak. (*FUSE*) *Far Ultraviolet Spectroscopic Explorer.*
[b] Blue: 3880–5040 Å; red: 5733–6896 Å.
[c] 1200 s exposure times.
[d] 1000 s exposure times.

image, and then applying a preliminary velocity correction to shift each image onto the spectra with the strongest emission lines. All of the flattened spectra were then combined with the routine SCOMBINE using a logarithmic wavelength scale. The heliocentric velocity for the template was removed for use in FXCOR (which automatically applies a heliocentric correction). The original flattened spectra were then run through the FXCOR package, which outputs the observed velocities for each spectra relative to the template. These observed velocities were then used to refine the preliminary velocity corrections and produce an improved template. This refining procedure was repeated, typically twice, until output velocities did not change significantly with each improved template. Radial mean velocities from this iteration procedure yielded uncertainties typically of 3 or 4 km s^{-1} (see Fig. 2), for those spectra in which the emission lines are strong.

2.2. *Mayall Echelle Spectroscopic Observations*

High-dispersion measurements of the emission-line profiles were obtained on the NOAO 4 m Mayall telescope located at KPNO in 2002 February (see Table 2). The CCD echelle spectrograph instrument was used with a 58.5 groves mm^{-1} grating along with the 226-1 226 groves mm^{-1} cross-dispersal grating, having a first-order blaze at 6700 Å. The T2KB 2048 × 2048 24 μm CCD recorded the spectra from 4270–7467 Å with a typical resolution of 0.16 Å at a reciprocal dispersion of 0.079 Å pixel^{-1}. Exposure times of 1800 s produced typical S/N of 20. Standard IRAF routines were used to reduce the data. ThAr lamps were used for wavelength calibration and G191-B2B was used as a spectrophotometric standard (Massey et al. 1988).

2.3. *FUSE*

Far-UV (900–1180 Å) spectra of HS 1136+6646 were obtained on two separate occasions with the *Far Ultraviolet Spectroscopic Explorer* (*FUSE*) satellite. The *FUSE* mission and its spectrographs, which achieve spectra resolutions of $\lambda/\Delta\lambda \sim 20,000$, are described in Moos et al. (1997). The observations of HS 1136+6646 (see Table 2) include a 2001 January 12 Cycle 2 *FUSE* observation (B053080100) under a program to investigate DAO and H-rich planetary nebulae central stars (PI: M. A. Barstow) and an observation obtained on 2002 January 29, as an observatory supplementary target (S60106061000). The 2001 observations consisted of two 3225 s exposures, separated in time by 100 minutes. The 2002 observations were continuous but divided into two consecu-
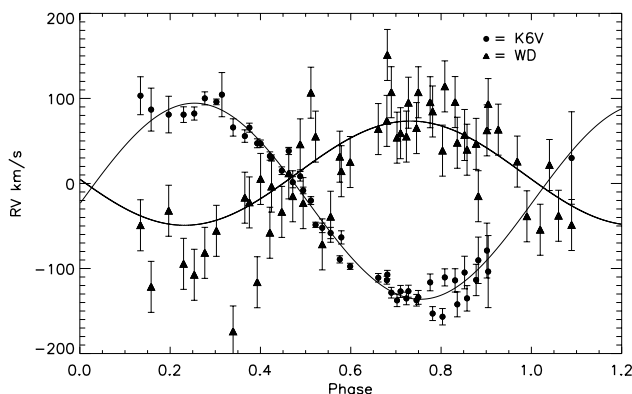

Fig. 2.—Folded radial velocities for both components, phased with a period of 0.83607 days.
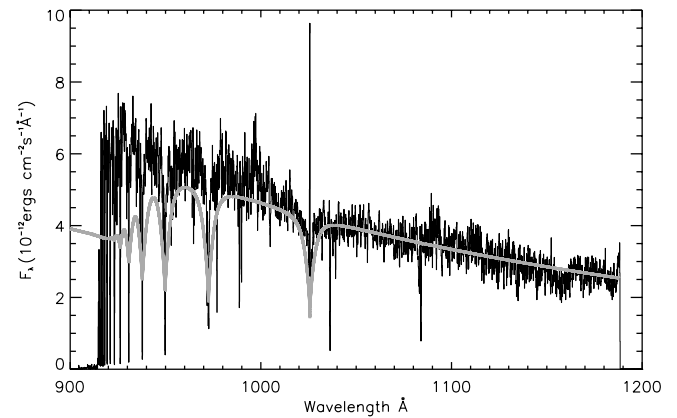

Fig. 3.—*FUSE* spectrum of HS 1136+6646 along with a $T_{\rm eff} = 110,000$ K, $\log g = 7.0$ model. Note the strong continuum that continues up to the Lyman limit without any roll-off.

tive 3939 s exposures. Both of the observations were obtained through the large (LWRS, $30'' \times 30''$) aperture in time tagged (TTG) mode.

Data from the 2001 and 2002 observations have been reduced using the most recent available version of the *FUSE* data reduction software (CALFUSE ver. 2.4). Extracted spectra from each of the four instrumental channels (separate optical paths consisting of different combinations of mirrors and gratings) and the two instrumental sides (independent microchannel plate detectors) were extracted. The resulting eight spectra were combined into a single continuous spectrum as follows. First, the spectra were compared and scaled in flux to match the observed flux in the LiF1 channel over the 1050–1070 Å range, since this wavelength region is common to all four channels. Second, the spectra were resampled onto a common uniform wavelength scale with increments of 0.05 Å, which approximate the instrumental spectra resolution. Mutual alignment of the component spectra was achieved with respect to interstellar absorptions features. Third, for each exposure, a single composite spectrum was produced by a co-addition process that weighted the fluxes with respect to the S/N in each spectral region. Photospheric features in the spectra corresponding to each exposure were measured and apparent stellar velocities relative to the interstellar medium (ISM) velocity were obtained. A final aggregate spectrum was also produced by Doppler shifting each of the exposures into the laboratory velocity frame using its measured relative stellar velocity. This aggregate spectrum, which has an S/N ~ 50 near 1000 Å, is shown in Figure 3.

The most striking feature of the HS 1136 *FUSE* spectra is the clear presence of the O vi $\lambda\lambda$1032, 1036 resonance doublet (see Fig. 4). Barstow et al. (2001) determined that temperatures in excess of 56,000 K are required to produce observable O vi lines in DA stars having nonstratified atmospheres. An extensive set of recent (2003 May) *FUSE* observations covering an entire orbit of HS 1136 also exist. A full analysis of the 2003 May observations will be reported in a future paper, although preliminary results are reported in this work.

3. PHOTOMETRIC OBSERVATIONS

3.1. *SARA Photometry*

UBVRI observations were obtained with the SARA 0.9 m automated telescope at Kitt Peak in Arizona. Both differential
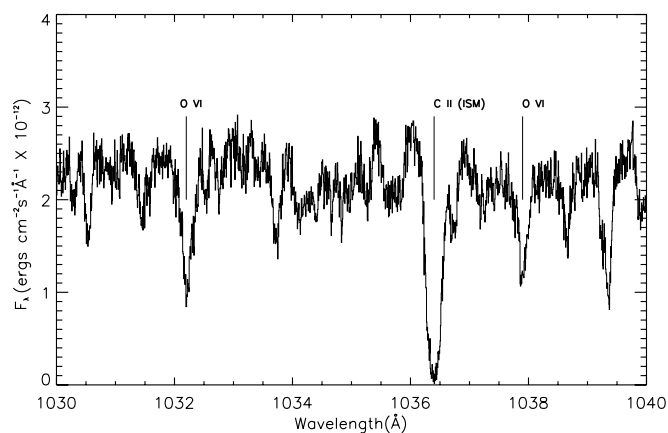
Fig. 4.—Portion of the 2002 *FUSE* spectrum of HS 1136+6646 showing the O VI stellar lines along with a C II interstellar line.

time-series and absolute photometry was obtained on several nights between 2002 March and June and between 2003 March and May (see Table 3) by both on-site and remote-access observers. Images were collected using an Apogee AP7p camera with a back-illuminated SITe SIA 502AB 512×512 pixel CCD. The pixels are 24 μm square, corresponding to $0\farcs73$ at the telescope focal plane. Read noise and gain for the camera are about 12.2 e^- (rms) and 6.1 e^- ADU^{-1}, respectively.

Duty cycle times were typically 25–35 s for the time-series work, including a readout time of $\sim$5 s. Sky flats and dark and bias exposures were taken every night. All data were calibrated and reduced using standard IRAF routines. Differential magnitudes were obtained using a brighter comparison star in the CCD field of view.

3.2. *JKT Photometry*

Intensive photometric monitoring of HS 1136 was also carried out by two of us (M. R. B. and S. A. G.) over five nights in 2002 February with the 1.0 m Jakobus Kapteyn Telescope (JKT) on La Palma. The JAG-CCD system was used with a SITe2 detector. This device has 2048×2048 24 μm

pixels and an image scale of $0\farcs33$ pixel^{-1}, giving an approximately $10' \times 10'$ field of view. Observations were made for up to $\sim$9 hr each night, through either a Harris *B*, *V*, or *R* filter. The exposure time for each individual frame was 40 s. Combined with the fast readout time of just over 1 minute, this gave a duty cycle of $\sim$2 minutes. Full details are given in Table 4. Standard calibrations such as sky flats and bias frames were also obtained each night.

Data reduction was carried out using standard Starlink software routines (e.g., FIGARO, Shortridge et al. 2001). Aperture photometry was performed using the PHOTOM package (Eaton, Draper, & Allen 2000). Differential magnitudes were then calculated with respect to a brighter comparison star in the CCD field of view.

Additional short photometric observations of HS 1136 were also made from the JKT by three of us (M. R. B., S. A. G., and C. S. B.) during 2002 May 12–19 and May 26–June 2, to help to unambiguously determine the binary orbital period. Typically, a set of five to ten 40 s exposures was made through a *V* filter each night. Data reduction was performed in a manner identical to that described above.

3.3. *UH 2.2 m Photometry*

CCD photometry of HS 1136 was obtained on 2003 April UT at the University of Hawaii 88 inch (2.25 m) telescope located on Mauna Kea. The observations were made with the OPTIC CCD camera using the newly implemented "video mode" for high-speed CCD photometry (Howell et al. 2003). Integrations of 30 s in a standard *V* filter were obtained from 8:30 to 10:45 UT and three local stars of similar brightness were used as comparisons for the differential photometry. HS 1136 was placed on the standard system using observations of the photometric standard fields near PG 1047+694 and PG 1528+062 (Landolt 1992). The CCD photometry yielded a *V*-band magnitude of 13.63 ± 0.03 at an orbital phase of about 0.25.

3.4. *2MASS Photometry*

Infrared photometry of HS 1136 was obtained from the Two Micron (2MASS) All-Sky Point Source Catalog. The resulting magnitudes are $J = 12.314 \pm 0.021$, $H = 11.695 \pm 0.024$,

TABLE 3
Log of Photometric Observations

Date	MJD Start (JD − 2,450,000)	MJD End (JD − 2,450,000)	Telescope[a]	Bands	No. Frames
2002 Mar 27	2360.698148	2361.037407	SARA	*V*	723
2002 Apr 8......................................	2372.643831	2373.025324	SARA	*V*	571
2002 Apr 17....................................	2381.877269	2382.016227	SARA	*V*	299
2002 May 16–18.............................	2410.935729	2412.904575	JKT	*BVR*	12 *V*, 2 *B* and *R*
2002 May 23....................................	2417.647118	2417.925058	SARA	*UBVRI*	59 *V*
2002 May 28–31	2422.870693	2426.912329	JKT	*V*	42
2002 Jun 07	2432.655880	2432.831655	SARA	*UBVRI*	48 *V*
2003 Mar 21	2720.624375	2721.019988	SARA	*V*	799
2003 Mar 22	2721.615058	2722.037674	SARA	*V*	756
2003 Mar 23	2722.871736	2722.799479	SARA	*V*	752
2003 Apr 08....................................	2737.84757	2737.93868	OPTIC/UH88	*V*	110
2003 May 25....................................	2784.670671	2784.846204	SARA	*V*	492
2003 May 26....................................	2785.746435	2785.896933	SARA	*V*	374
2003 May 27....................................	2786.665949	2786.870926	SARA	*V*	490

[a] (SARA) Southeastern Association for Research in Astronomy telescope at Kitt Peak; (JKT) Jacobus Kapteyn Telescope at La Palma; (OPTIC/UH88): University of Hawaii 88 inch (2.25 m) telescope at Mauna Kea.

TABLE 4
SUMMARY OF 2002 FEBRUARY JKT OBSERVING RUN

UT Date	Filter	Exposure Time (s)	Duration (hr)	No. Frames	Conditions
2002 Feb 34............	V	40	7.0	214	Photometric, seeing 1″3
2002 Feb 4/5............	R	40	4.2	129	Observed through cirrus, seeing 1″
2002 Feb 5/6............	B	40	5.8	179	Cirrus, seeing variable, 1″2 –4″
2002 Feb 6/7............	B	40	8.8	270	Not photometric, seeing 2″
2002 Feb 7/8............	R	40	6.9	181	Not photometric, seeing 3″–5″

and $K = 11.543 \pm 0.021$, from which the corresponding colors can be derived, $J-H = +0.619 \pm 0.032$ and $H-K = +0.152 \pm 0.032$. These 2MASS magnitudes, colors, and uncertainties are used to estimate the apparent spectral type of the main-sequence component of the binary system.

4. ANALYSIS

4.1. Radial Velocities

The radial velocity curves for both components of the HS 1136 system are shown in Figure 2. The apparent velocities of the K star are derived directly from the unresolved Bok CCD spectra of the emission lines. It should be noted here that the Mayall echelle spectra reveal these lines to be surprisingly broad and to consist of asymmetric centrally reversed line profiles (see § 4.6). Thus, the velocities in Figure 2 pertain to centroids of the emission lines. Since these emission lines may contain nonphotocentric components (see § 4.6), they may also possess possible nonorbital biases.

The estimate of the K velocity for the white dwarf, based solely on the weak He II λ4686 line, is $K_{WD} = 61 \pm 10 \text{ km s}^{-1}$. A significantly better estimate, however, is available from a preliminary analysis of a recent 2003 May *FUSE* observation of HS 1136, which covered nearly a full orbital cycle. A complete analysis of the 2003 May *FUSE* observations will be reported elsewhere; however, we will use the preliminary *FUSE* value of $K_{WD} = 69 \pm 2 \text{ km s}^{-1}$ in lieu of our ground-based value.

All of the emission lines from the narrow irradiation component are observed to disappear near the inferior conjunction and remain undetectable for ~15% of the total orbit. At this orbital phase, the observed spectrum is effectively a composite of the white dwarf and the dark side of the K star. A

DA+dM4 binary system with similar emission-line behavior, PG 1224+309, was studied by Orosz et al. (1999), who determined an inclination of $77° \pm 7°$. The 0.25 day period PG 1224+309 system is only a few degrees away from giving rise to an eclipse, but the emission lines are seen throughout the entire orbital phase. Emission-line disappearance in the HS 1136 system therefore suggests a relatively high inclination.

Measurements of the equivalent widths of the spectral lines show a modulation at the same orbital period, but with a one-quarter phase difference (see Fig. 5). This difference is consistent with the notion of the reflection effect giving rise to the narrow peaks of the emission lines. The preliminary mass ratio $q = M_{K7V}/M_{WD}$ is estimated from the ratio of the K velocities giving a value of 0.60.

4.2. Photometry

UBVRI photometric observations revealed a time-dependant sinusoidal variation of the light emission from HS 1136 due to the orbital motion in the binary system and the reflection effect. From the reflection effect, the hemisphere of the secondary star facing the hot white dwarf is optically brighter than the outward-facing hemisphere. As the two stars orbit one another, the observed *UBVRI* fluxes vary with the percentage of the illuminated hemisphere seen.

In addition to the large amplitude photometric variations associated with the orbit, low-amplitude photometric variations of a much shorter period are also observed. These short-period modulations have a period of 113.13 minutes, a half-amplitude of ~0.0093 mag, and can be clearly seen in the orbital photometric light curve of Figure 6. They appear to be present in all observations and to be independent of orbital phase. They are coherent from night to night and, as seen from preliminary modeling (Fig. 7), can almost certainly be phased
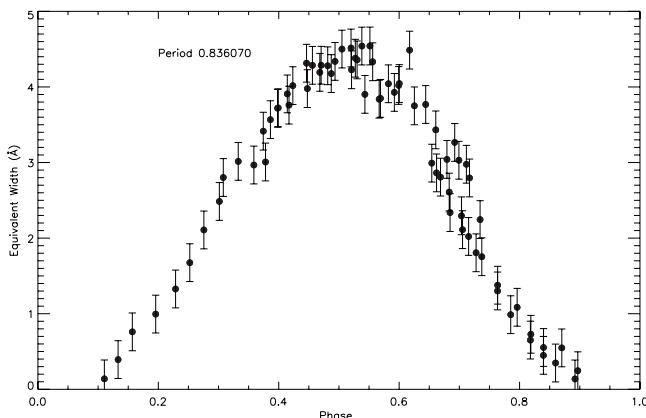

FIG. 5.—Mean spectroscopic emission line equivalent widths as a function of orbital phase (see discussion in text). Data for 2001 March, May, December and 2002 March are phased with a period of 0.83607 days.
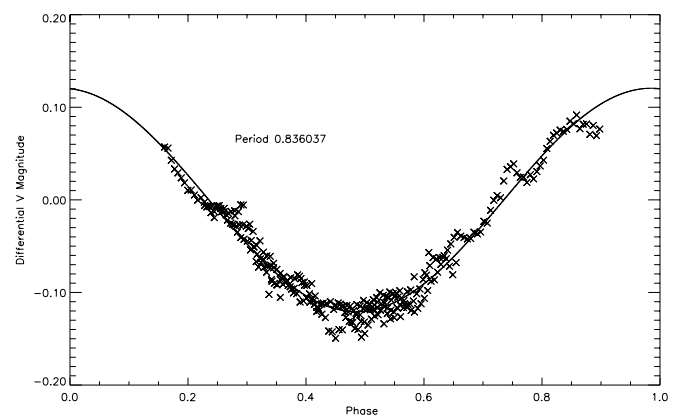

FIG. 6.—Resampled *V*-band SARA photometry phased after subtracting a sine curve fit to the small modulations. Phase dispersion minimization fits result in an orbital period of 0.83604 days.
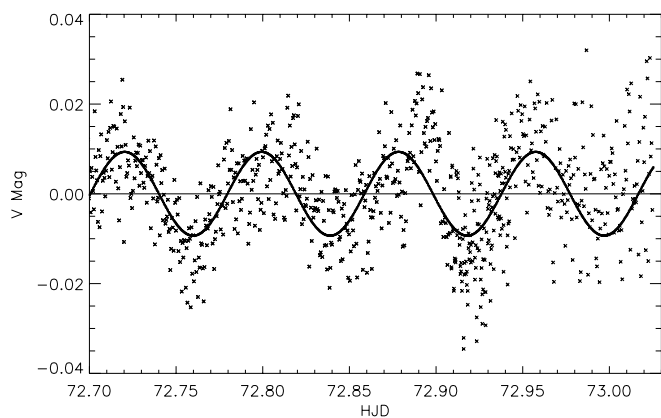
FIG. 7.—Low-amplitude 113 minute modulation seen in the residuals of the SARA photometric V-band light curve. The modulation is believed to be related to the rotation of a magnetic spot on the white dwarf.
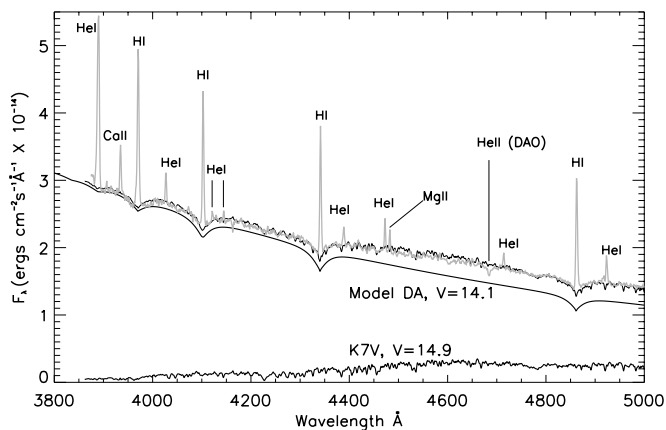

FIG. 8.—Models of the HS 1136+6646 components and composite spectra overplotted with the Bok spectroscopic data (gray) near the superior conjunction.

over much longer periods with sufficient data. In Figure 7 we show a residual light curve, after removal of the orbital variations, compared with a best-fitting sine wave having a period of 113.13 minutes and a semiamplitude of 0.0093 mag. There are indications that the wave form is doubly sinusoidal, or that the amplitude may vary, but night-to-night matching of the photometry makes departures from a pure sine wave difficult to characterize from the present data. Handler (1998) searched for short-period pulsations in HS 1136 using high-speed relative photometry. No evidence of short-period variations were observed but the short duration of the observation (76 minutes) together with other variations seen and the low-frequency filtering of the data would have made it difficult to detect any variations of the type we report. The low-amplitude, 113 minute modulations are presumed to originate with the hot white dwarf and to be associated with either a rotational photometric modulation due to a magnetic spot or pole on the white dwarf's surface. Alternative explanations such as pulsational instability in the white dwarf or rotational modulations of the K star are less likely. The observed 113 minute period of the modulations is well outside the known range

of degenerate star pulsations and is too short for any stable rotation of the K star.

4.3. Determination of Orbital Ephemeris

The orbital period was determined using the χ^2-based phase dispersion minimization (PDM) technique as described in Stellingwerf (1978). The V-band photometric data was supplemented with the emission-line equivalent width data (see Table 5) to achieve better accuracy. The equivalent widths of the emission lines were measured from the five brightest H I and He I lines (see Fig. 8). An average strength for these five lines computed for each spectrum was used in the PDM technique, yielding an orbital period of 0.83607 ± 0.00003 days using all of the spectroscopic ground-based data (see Table 2; Fig. 5). Since the 113 minute modulations are not necessarily related to the orbital motion, phasing the V-band data alone led to systematic errors in determining the period, since the PDM couples to the small variations. In order to avoid this systematic error, a preliminary fit of the small modulations with a cosine function (see Fig. 7) was made and

TABLE 5
BOK EQUIVALENT WIDTH MEASUREMENTS OF EMISSION LINES AT ORBITAL PHASE = 0.5

Species	Wavelength (Å)	Continuum (ergs cm^{-2} s^{-1} Å^{-1})	Flux (ergs cm^{-2} s^{-1} Å^{-1})	Equivalent Width (Å)	GFWHM[a] (Å)
H I	3970.072[c]	2.362×10^{-14}	9.958×10^{-14}	−4.22	3.526
H I	4101.740	1.968×10^{-14}	7.439×10^{-14}	−3.78	3.287
H I	4340.470	1.665×10^{-14}	7.385×10^{-14}	−4.44	3.124
H I	4861.330	1.119×10^{-14}	6.008×10^{-14}	−5.37	3.600
He I and H I	3888.650	2.615×10^{-14}	9.188×10^{-14}	−3.51	3.623
He I.....................	4026.191	2.241×10^{-14}	1.738×10^{-14}	−0.77	3.019
He I.....................	4120.820	2.190×10^{-14}	6.686×10^{-15}	−0.31	3.264
He I.....................	4143.760	2.200×10^{-14}	5.022×10^{-15}	−0.23	2.378
He I.....................	4387.929	1.562×10^{-14}	7.074×10^{-15}	−0.45	2.658
He I.....................	4471.479	1.463×10^{-14}	1.358×10^{-14}	−0.93	2.626
He I.....................	4713.146	1.274×10^{-14}	6.121×10^{-15}	−0.48	2.690
He I.....................	4921.931	1.180×10^{-14}	1.265×10^{-14}	−1.07	3.173
Ca II.....................	3933.660	2.478×10^{-14}	2.685×10^{-14}	−1.08	3.016
C II.....................	4267.260	1.702×10^{-14}	6.312×10^{-15}	−0.37	2.583
Mg II.....................	4481.245[b]	1.464×10^{-14}	8.717×10^{-15}	−0.60	2.258

[a] FWHM based on a Gaussian fit.
[b] Includes the Ca II λ 3968.470 line, explaining a relatively larger equivalent width and GFWHM as compared to the other hydrogen lines.
[c] Blend of 4481.160 and 4481.330.

subtracted from the V-band photometric data. This procedure was performed by first fitting the orbital variations with a cosine function of the form

$$V_{\mathrm{mag}}(t) = V_0 \cos\left(2\pi\frac{t - T_0}{P}\right) + \langle V\rangle, \qquad (1)$$

where V_{mag} is the observed V magnitude, V_0 is the amplitude of the light curve, and $\langle V\rangle$ is the mean magnitude. The fit was then subtracted from the photometric data before determining the period. Although some small modulations are still present, a period of 0.83604 ± 0.00004 days is obtained from the PDM fit. This closely matches the period obtained with spectroscopic equivalent width data (see Fig. 6). The radial velocity data agrees well with this period, as shown in Fig. 2, which overplots the radial velocity data as sinusoids of the form

$$V_{\mathrm{WD}}(t) = \gamma' + K_{\mathrm{WD}} \sin\left(2\pi\frac{t - T_0}{P}\right), \qquad (2)$$

for the white dwarf, and

$$V_{\mathrm{K7V}}(t) = \gamma + K_{\mathrm{K7V}} \sin\left(2\pi\frac{t - T_0}{P}\right), \qquad (3)$$

for the secondary star, with the orbital parameters as listed in Table 1, where K_{WD} and K_{K7V} are the K velocities, P is the orbital period, and T_0 and t are, respectively, the epoch and time; γ and γ' are, respectively, the system gamma velocity and the algebraic sum of the system velocity plus gravitational redshift of the white dwarf.

4.4. Properties of the White Dwarf

In principal, it is possible to independently estimate the effective temperature and gravity of a hot white dwarf such as HS 1136 from a detailed analysis of both the Balmer and Lyman line profiles. However, in the case of HS 1136, the Balmer lines are contaminated both by the continuum from the secondary star and the emission lines. We have attempted to minimize this contamination by the following procedure.

Optical spectra obtained near the orbital inferior conjunction (see Fig. 9) with the Bok telescope were used to extract a characteristic white dwarf spectrum. In order to remove the K star from the composite flux as accurately as possible, a template spectrum of the K7 V star BD $+46°1635$ was obtained with the Bok telescope on 2003 March 23. This ensured that the template K star spectrum had the same resolution, dispersion, and wavelength range as the HS 1136 spectra at inferior conjunction. Shortward of 4000 Å, the flux of HS 1136 is dominated by the hot white dwarf, making it possible to accurately flux calibrate an assumed *preliminary* model of the white dwarf ($T_{\mathrm{eff}} = 50{,}000$ K, $\log g = 8.0$). The template K7 V star was then flux-calibrated so that the composite model flux corresponded to the observed levels of the HS 1136 spectra. A preliminary model white dwarf spectrum was then obtained by subtracting the spectrum of the correctly flux-calibrated K7 V star from the HS 1136 spectra at inferior conjunction. This white dwarf spectrum was then fitted with a grid LTE, pure-hydrogen model stellar atmospheres produced by TLUSTY (Hubeny & Lanz 1995).

A final set of white dwarf parameters was obtained by the following iterative procedure. A synthetic white dwarf spectrum was generated from fitted T_{eff} and $\log g$ values, which was then used to rescale the subtracted K7 V template
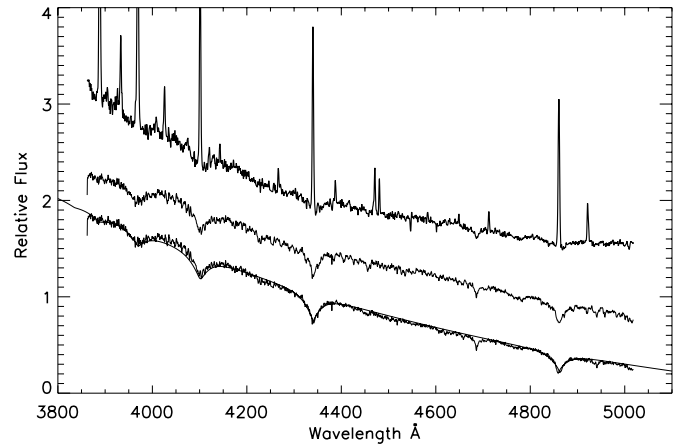

Fig. 9.—Bok 2.4 m emission-line spectra at the superior conjunction (*top*) compared with the spectrum at the inferior conjunction (*middle*) and the extracted white dwarf spectrum (*bottom*). The best-fitting model white dwarf spectrum of $T_{\mathrm{eff}} = 70{,}000$ K and $\log g = 7.75$ is overplotted on top of the extracted white dwarf spectrum.

spectrum. The new white dwarf spectrum was then refitted and a new set of white dwarf parameters determined. A final set of parameters corresponding to $T_{\mathrm{eff}} = 70{,}000 \pm 5000$ K and $\log g = 7.75 \pm 0.25$ was achieved after several iterations. This final model is shown in Fig. 9. Note that the fitting procedure employed normalized individual Balmer profiles, thereby minimizing any bias associated with the sloping spectral energy distribution. Best results were obtained from the Hγ and Hδ lines, suggesting that not all of the K7 V flux was properly subtracted from the composite spectra.

In principal, it is also possible to use the H I Lyman series lines to estimate the T_{eff} and $\log g$ of HS 1136. Barstow et al. (2003) have extensively investigated the relationship between Balmer line estimates and those derived from the *FUSE* Lyman lines spectra for a set of 16 DA white dwarfs. In general, they find very good agreement for stars with temperatures below $\sim50{,}000$ K and increasingly wide divergence for stars at higher temperatures. The sense of the difference in temperatures found by these two methods is that Lyman line temperatures began to exceed the Balmer line temperatures at $\sim50{,}000$ K, increasing to a discrepancy of 6% to 10% higher by 60,000 K. The corresponding correlation for gravities shows a good agreement between Lyman and Balmer results. There is a weak indication of higher Lyman line gravities for the very hottest stars, but this is based only on two stars with large error bars. At present, we can suggest no explanation for the differences between the two methods nor is there a clear indication of which method, Lyman or Balmer, provides the best estimate of effective temperature for the hottest H-rich white dwarfs.

Keeping the results of Barstow et al. (2003) in mind, we fitted the Lyman lines for HS 1136 in a χ^2 minimization technique similar to that of Barstow et al. (2003). We find $T_{\mathrm{eff}} = 110{,}000$ K and $\log g = 7.0$–7.5 using the 2001 and 2002 *FUSE* observations. However, this fit is very unsatisfactory (see Fig. 3) and is also incompatible with the strong continuum that continues up to the Lyman limit with no discernible roll-off at the convergence of the Lyman series. Models indicate that a much higher effective temperature is necessary to match the spectral energy distribution shortward of 950 Å and the Lyman limit. Clearly, the Lyman line temperature and the far-UV (FUV) energy distribution are incompatible with our results for the Balmer line fits. Nevertheless, both Balmer

and Lyman analysis place HS 1136 among the hottest stars considered by Barstow et al. (2003) and among the hottest H-rich white dwarfs known. Although we are presently unable to reconcile the Balmer and Lyman line results, we will adopt the Balmer line parameters $T_{\mathrm{eff}} = 70,000$ K and $\log g = 7.75$ as a good match to the white dwarf at optical wavelengths and use these results in the discussion that follows.

An estimate of the mass and thermal age of the white dwarf can be obtained from its Balmer line temperature and gravity. Using the thermally evolved models of Wood (1995), we find a mass of $M_{\mathrm{WD}} = 0.63 \pm 0.05 \, M_{\odot}$ and a thermal age of $(8.2 \pm 0.7) \times 10^5$ yr for the white dwarf. From synthetic photometry of Bergeron et al. (1995) we find a corresponding M_v of 8.5 for the white dwarf.

In addition to the temperature and gravity, the optical spectrum of the white dwarf can be used to estimate the photospheric He abundance of the white dwarf. The measured equivalent width of the He II $\lambda 4686$ line is 32 mÅ, which for a 70,000 K, $\log g = 7.75$ white dwarf corresponds to a He abundance of He/H $\sim 2 \times 10^{-3}$.

4.5. Properties of the K Star

The approximate spectral type of the main-sequence companion can be best estimated from the observed 2MASS *JHK* colors in § 3.4. These infrared colors can be compared with the intrinsic main-sequence colors of K dwarfs given in Bessell & Brett (1988). After transforming the Bessell & Brett colors to the equivalent 2MASS colors using the color transformations of Carpenter (2001), the observed 2MASS colors correspond the range of spectral types of K4–M0 V with an apparent visual magnitude of 14.34–15.27. We will adopt K7$^{+4}_{-2}$ V. This estimate is quite consistent with the spectroscopic determination of Heber et al. (1996), based on the atomic and molecular features seen in their red spectrum of the star as well as our modeling of the optical continuum near superior and inferior conjunction, which assumed a K7 V secondary (Pickles 1998) and a 70,000 K, $\log g = 7.75$ white dwarf (see Fig. 8). It should be noted that the 2MASS data were obtained at a phase of 0.22 ± 0.05, which corresponds to the mean of the *V*-band photometric orbital variations. Second, this also assumes that the main-sequence star can be characterized by its *JHK* colors and is not over-luminous as is the case with V 471 Tau (O'Brien, Bond, & Sion 2001).

4.6. Emission-Line Profiles

Observations of HS 1136 were obtained on 2003 January 03–04 with the 4 m Mayall telescope yielding five spectra that cover an orbital phase range from 0.05 to 0.45. These echelle spectra, which fully resolve the emission lines, revealed lines that are unexpectedly broad and asymmetrically double-peaked (see Fig. 10). Neither of these aspects are obviously compatible with emission arising solely from the irradiated stellar photosphere of the K7 V star. The three hydrogen emission lines, Hα, Hβ, and Hγ, have FWHM of 5.34, 3.15, and 2.84 Å, respectively. Line broadening due to differential orbital motion during the 1800 s exposure and thermal Doppler broadening at 7000 K explain the width of the He I, He II, Ca II, and Mg II lines, but not those of the broader H I lines. Unlike the other emission lines, the hydrogen lines clearly show the double-peaked feature. Figure 10 shows the development of the Hα emission line as a function of orbital phase over almost half a cycle. As the strength of the emission grows, there is a pronounced asymmetry
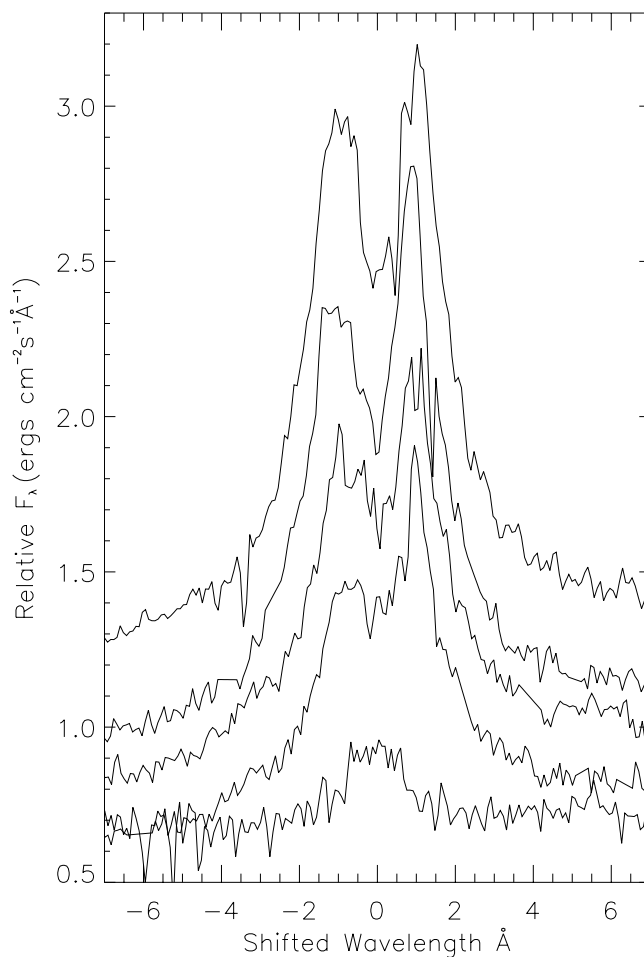

Fig. 10.—Mayall 4 m Hα emission-line profiles from the inferior conjunction (*bottom*) to the superior conjunction (*top*). The corresponding phases from bottom to top are 0.05, 0.25, 0.28, 0.39, and 0.45.

between the two peaks, which tends to diminish near the superior conjunction.

One possible explanation for the double-peaked emission-line structures observed in HS 1136 is that they are due to an accretion disk. The aspects of the lines that lend themselves to this idea are the asymmetric nature of the peaks and the ~ 300 km s^{-1} widths. Under this assumption, we would assign the higher, narrow peak to irradiation from the K7 V star with the underlying (now symmetric) double-peaked structure due to a disk of captured (wind) material orbiting the white dwarf. Taking the orbital parameters we have derived in this paper, the line widths observed place the disk far from the white dwarf near a radius of $0.7R_L$, where R_L is the Roche lobe radius, and its structure would have to be very optically thin or completely evaporated (a Strömgren sphere) in its interior; a very ringlike disk. The argument against an accretion disk is that we note the large decrease in the line strengths and their symmetric nature at phase 0.05, requiring a nearly complete eclipse of the disk by the K7 V star.

The double-peaked emission line structure may also be attributed to Stark broadening analogous to BE UMa, in which case the lines are formed deep in the atmosphere of the K7 V star (Ferguson & James 1994). Emission lines in BE UMa from elements heavier than hydrogen, such as C II, C III, and N III, are formed higher up in the atmosphere and thus are not as broad as the Balmer lines. Such would be the case with HS 1136 were

TABLE 6
Similar Post-CE Systems

System	Period (days)	a ($R_\odot$)	Components	$T_{\rm eff}$ (K)	WD Mass ($M_\odot$)	Post-CE Age (yr)
BE UMa.................................	2.291	7.5	sdO/DAO+K5 V	105,000	0.7	10^4
HS 1136+6646........................	0.836	3.7	DAO+K7 V	70,000	0.64	10^5
V 471 Tau..............................	0.521	3.3	DA+K2 V	34,000	0.84	10^7

the He I, He II, Ca II, and Mg II lines are not as broad nor observed to be double-peaked. Unlike HS 1136, however, the double-peaked emission-line profiles of BE UMa are reportedly symmetric throughout the orbital cycle. The asymmetry of the Balmer lines in HS 1136 raises doubts about the validity of the Stark broadening mechanism and leaves a satisfactory explanation of the nature of the emission lines elusive.

4.7. Binary Components

With a known preliminary mass ratio of $q = 0.6$ (§ 4.1), we employ two scenarios in order to estimate a consistent set of binary system parameters. In this manner we can investigate which assumptions made in estimating the parameters are consistent with other observed features, such as emission-line disappearance. In the first scenario, we assume a white dwarf mass based on Balmer line fits for $T_{\rm eff}$, log g, and a K star that has a radius *twice* that of a K7 V zero-age main-sequence (ZAMS) star. This scenario is based on the possibility that HS 1136 resembles other very young CE systems, such as BE UMa, in which the main-sequence companion has been heated by the accretion of matter during the CE phase (see Schreiber & Gänsicke 2003). A white dwarf mass of $M_{\rm WD} = 0.63\ M_\odot$ and age of 7.7×10^5 yr is adopted from the synthetic photometry of Bergeron et al. (1995), based on a $T_{\rm eff} = 70,000$ K and log $g = 7.75$ DA white dwarf. Since the radial velocity profile of the K7 V star is derived from observations of the emission lines, the observed value of $q = 0.6$ represents an upper limit. In order to shift the apparent radial velocity from the center of light to the center of mass, a correction of $+16$ km s^{-1} to the radial velocity is needed (see Orosz et al. 1999 for velocity correction discussion and technique). This estimate assumes a radius of 0.79 $R_\odot$ and mass 0.38 $M_\odot$ (Pickles 1998) for the secondary star, which is uniformly illuminated over one hemisphere, along with a q value of 0.6. With an observed value of $K_{\rm K7V} = 115$ km s^{-1}, the "K-corrected" value is then 131 km s^{-1}. The new q value is then 0.53 corresponding to a secondary star mass of $M_{\rm dK} = 0.33\ M_\odot$. Kepler's third law then gives the orbital separation a,

$$a^3 = G(M_{\rm WD} + M_{\rm dK})(P/2\pi)^2, \qquad (4)$$

and the inclination follows from

$$\sin^3 i = \frac{PK_{\rm dK}(K_{\rm WD} + K_{\rm dK})^2}{2\pi GM_{\rm WD}}, \qquad (5)$$

where G is the gravitational constant and the other parameters are listed in Table 1. We find $a = 3.7\ R_\odot$ and $i = 64° \pm 6°$. Eclipses have not been observed, placing an upper limit on the inclination of $i < 80°$, based on the parameters listed in Table 1. This is consistent with the value given by equation (5).

In the second scenario it is assumed that the secondary component is a K7 V ZAMS star with a mass of 0.609 $M_\odot$ and a radius of 0.681 R$_\odot$. The K corrected value for $K_{\rm K7V}$ becomes

127 km s^{-1}, resulting in a q value of 0.54, which corresponds to a white dwarf mass of 1.12 $M_\odot$. Equation (4) then gives an orbital separation of 4.5 $R_\odot$, while equation (5) gives an inclination of $46° \pm 3°$. An inclination of $46°$ is too low for the emission lines to be associated with the reflection effect, and below a lower limit of $54°$ set with the known orbital period, $K_{\rm K7V} > 115$ km s^{-1}, $K_{\rm WD} = 69$ km s^{-1}, and a white dwarf mass 0.63 $M_\odot$, which is more reasonable. At such an angle, the lines would remain visible throughout the orbital cycle. In addition, the high white dwarf mass, 1.12 $M_\odot$, would imply a gravity of log $g > 8.5$, which is not consistent with either our Balmer or Lyman spectral analysis.

5. DISCUSSION

5.1. Parameters of the Binary System

The parameters found in the first scenario in § 4.7 require the K7 V star to be out of thermal equilibrium and the mass of the white dwarf to be around 0.6 $M_\odot$. A secondary star mass of 0.33 $M_\odot$ is not characteristic of a K7 V star, rather it indicates the secondary star may actually be an early-M star. This lower mass is clearly at odds with the observed luminosity as well as the spectral typing of the secondary as a K7 V star and is further evidence that the secondary may be overly luminous. There are several reasons for believing this first scenario is more likely than the second. First, there are four binary systems closely related in temperature to HS 1136 that have measured orbital parameters: UU Sge, V477 Lyr, KV Vel, and BE UMa (Schreiber & Gänsicke 2003). All of these binary systems have a hot (>60,000 K) primary component indicating the systems are very young. All have a secondary star with radii inflated by a factor of ~2. The thermal timescale of the envelope of the K7 V star is much higher than the cooling time of the white dwarf (~7.7×10^5 yr) following the accretion of matter during the CE phase for the HS 1136 system. This supports the notion that the K star is out of thermal equilibrium. The second scenario, which results in a higher white dwarf mass, would only strengthen the above argument since the cooling time would be shorter. The narrow-peak emission-line disappearance near orbital phase zero is another reason to favor the first scenario. The inclination derived in the second scenario is nearly $20°$ lower than in the first. If the binary system were in such a low-inclination orbit, a nontrivial fraction of the secondary star's irradiated hemisphere would always be visible, and the emission lines would always be present.

5.2. Age of the Binary System

The cooling time of the hot white dwarf is on the order of 7.7×10^5 yr, which indicates that the HS 1136 system has just recently emerged from the post–CE phase (see Table 6). This system can test the origins of CE evolution and help determine such parameters as the efficiency of the CE process and whether post-CE secondaries satisfy a normal main-sequence

mass-radius relation (Orosz et al. 1999). HS 1136 is similar to the well-known systems Feige 24 and V 471 Tau, which are hot DA stars with dM2 and dK2 companions, respectively. Feige 24 shows a well-studied reflection effect while the DA in V471 Tau is too cool relative to its main-sequence companion to produce an observable reflection effect.

5.3. *Similar Post–CE, Pre-CV Stars*

It is of interest to compare HS 1136 with two other well-observed systems that, in many ways, appear to bracket it. These two systems are BE UMa (Ferguson et al. 1999 and references therein) and V 471 Tau (O'Brien et al. 2001 and references therein). All of these systems appear to have a post-CE origin and to contain a hot degenerate star with a main-sequence K star. In Table 6 we list the system parameters and the characteristics of the degenerate stars. Since both BE UMa and V 471 Tau are eclipsing systems, the stellar parameters of the two components are relatively well determined.

Like HS 1136, BE UMa exhibits a very strong reflection effect, both in the continuum and emission lines. The latter exhibits a host of first- and second-ionization stages of CNO species as well as Si and Al. The key aspect of BE UMa is the high luminosity of the degenerate star, which has led Ferguson et al. (1999) to classify it as a borderline sdO/DAO star. In contrast, although the effective temperatures of the degenerate stars in HS 1136 and BE UMa are similar, the DAO star in HS 1136 is not nearly as luminous or dominant compared to its main-sequence companion. Ferguson et al. (1999) estimate the gravity of the degenerate star in BE UMa to be 6.5, while the composite spectrum of HS 1136 can be used to place a lower limit of 7.0 on the gravity of the DAO.

V 471 Tau, on the other hand, is almost completely dominated by the K star and shows no detectable reflection effect. However, low-amplitude variations, similar to the ones detected in HS 1136 (§ 4.2), have been reported in the soft X-ray in V471 Tau (Jensen et al. 1986) and in the EUV from the hot white dwarf GD 394 (Dupuis et al. 2000). In both cases these modulations are believed to be associated with the rotation of the white dwarf. In particular, the magnetic "spots" are thought to accrete high-z matter producing a nonuniform distribution of heavy elements on the stellar surface. Ellipsoidal variations cannot contribute to the main orbital photometric modulations seen in HS 1136, as the secondary does not fill its Roche lobe.

The K5 V secondary star of BE UMa is out of thermal equilibrium, resulting in a radius nearly twice that expected. This large radius is a result of the thermal timescale of the star's envelope being longer than the time since emerging from the CE phase (Ferguson et al. 1999). The thermal timescale for the K7 V star in HS 1136 is $\sim 10^6$ yr, which is more than the estimated age of 7.7×10^5 yr, leaving open the possibility that it, too, is not in thermal equilibrium and has an extended radius.

In Table 6 we also list the estimated post-CE ages for all three systems based on white dwarf cooling ages. In the case of BE UMa, the high luminosity of the degenerate star complicates the interpretation of its evolutionary status. It is clearly a very young system since Liebert et al. (1995) have detected a $3'$ nebula surrounding the star. For reasonable estimates of the expansion rate of the nebula, they find good agreement with the thermal age of the degenerate. V 471 Tau is clearly the oldest system of the three, but the thermal age of the DA is in apparent conflict with its being a member of the Hyades cluster (O'Brien et al. 2001).

5.4. *The Future Evolution of HS 1136+6646*

We have modeled the orbital evolution of HS 1136 using the parameters listed in Table 1. Specifically, we assume a white dwarf mass of 0.7 $M_\odot$ and a respective K7 V star mass of 0.61 $M_\odot$ and radius of 0.56 $R_\odot$. The initial period of the system was estimated to be 0.83 days. This period is somewhat longer then the present orbital period but less than a day, which would be typical of the progenitor binary. We have followed the orbital evolution of the system using the secular evolution model code described in Howell et al. (2001). We find that the present system will continue to evolve toward shorter orbital periods for approximately 1×10^9 yr. When the system reaches an orbital period of approximately 4.9 hr, the Roche lobe of the K7 V companion will contact the white dwarf surface and a high rate of mass transfer will commence. HS 1136 should then become a standard CV system. It is interesting to speculate that if the 113 minute modulation is in fact due to a magnetic spot on the surface of the white dwarf and if the magnetic field is strong enough (1–10 MG), then HS 1136 may be an incipient intermediate polar or DQ Her star. In DQ Her stars, the magnetic field of the white dwarf is too weak to create the well-defined accretion columns characteristic of the AM Her type systems. Such systems often form a partial accretion disk. By the time mass transfer begins, the white dwarf will have cooled to between 6000 and 7000 K and will no longer dominate the optical flux from the system. However, for a typical 5 hr orbital period cataclysmic variable, the white dwarf temperature is 30,000 K or more (Sion 1999). Apparently HS 1136 will reheat quickly once mass accretion begins.

6. CONCLUSIONS

HS 1136 offers a unique opportunity to study a recently evolved common-envelope (CE) system that is relatively bright and nearby. We have presented new spectroscopic and photometric observations that characterize the binary parameters of HS 1136. These observations also show HS 1136 to be the second youngest post-CE system known having emerged from its CE phase only $\sim 10^5$ yr ago. From analysis of the binary parameters, we find that HS 1136 has a K7V star that is out of thermal equilibrium. The photometric measurements reveal low-amplitude 113 minute modulations that are presumably due to the rotation of the white dwarf. Synthetic white dwarf model fits to the Balmer line profiles of the white dwarf in HS 1136 give a $T_{\rm eff} = 70,000$ K and $\log g = 7.75$. This temperature and gravity remain difficult to reconcile with the UV spectrum Lyman line results, $T_{\rm eff} = 110,000$ K and $\log g = 7.00$–7.5.

In 2003 May, HS 1136 was observed by the *FUSE* spacecraft. These UV observations provided nearly complete orbital coverage of the binary system and should allow a better determination of the white dwarf velocity curve. A preliminary value is cited in this work, as well as a very high S/N FUV spectrum of the white dwarf. Cycle 12 observations with the Space Telescope Imaging Spectrograph (STIS) are also planed with the *Hubble Space Telescope*. The echelle UV spectra expected from these observations should allow placement of the *FUSE* velocity for the white dwarf on an absolute scale and also provide a gravitational redshift for the white dwarf. Such observations will allow detailed modeling of the white dwarf photosphere and a determination of its heavy-element abundance. Studies of the low amplitude 113 minute modulations will also continue from the ground, using multiple

sights to obtain longer unbroken photometric series to better determine the waveform and hopefully to identify its source. A better understanding of the orbital-related changes in the components of the emission lines will result from echelle spectra that cover a full orbit.

REFERENCES

Barstow, M. A., Burleigh, M. R., Bannister, N. P., Holberg, J. B., Hubeny, I., Bruhweiler, F. C., & Napiwotzki, R. 2001, in ASP Conf. Ser., Vol. 226, 12th Euopean Conference on White Dwarfs, ed. J. L. Provencal et al.(San Francisco: ASP), 128
Barstow, M. A., Good, S. A., Burleigh, M. R., Hubeny, I., Holberg, J. B., & Levan, A. J. 2003, MNRAS, 344, 562B
Bergeron, P., Wesemael, F., & Beauchamp, A. 1995, PASP, 107, 1047
Bessell, M. S., & Brett, J. M. 1988, PASP, 100, 1134
Carpenter, J. M. 2001, AJ, 121, 2851
Dupuis, J., Chayer, P., Vennes, S., Christian, D. J., & Kruk, J. W. 2000, ApJ, 537, 977
Eaton, N., Draper, P. W., & Allan, A. 2000, PHOTOM: A Photometry Package (Starlink User Note 45.12; Chilton: Rutherford Appleton Lab.)
Ferguson, D. H., & James, T. A. 1994, ApJS, 94, 723
Ferguson, D. H., Liebert, J., Haas, S., Napiwotzki, R., & James, G. A. 1999, ApJ, 528, 866
Handler, G. 1998, A&A, 339, 170
Heber, U., Dreizler, S., & Hagen, H. J. 1996, A&A, 311, L17
Holberg, J. B., Sing, D. K., Barstow, M. A., & Good, S. 2001, Astron. Ges. Abstr. Ser., 18, No. P106
Howell, S. B., Everett, M. E., Tonry, J. L., Pickles, A., & Dain, C. 2003, PASP, 115, 1340
Howell, S. B., Nelson, L. A., & Rappaport, S. 2001, ApJ, 550, 897H

Hubeny, I., & Lanz, T. 1995, ApJ, 439, 875
Jensen, K. A., Swank, J. H., Petre, R., Guinan, E. F., Sion, E. M., & Shipman, H. L. 1986, ApJ, 309, L27
Landolt, A. U. 1992, AJ, 104, 340
Liebert, J., Tweedy, R. W., Napiwotzki, R., & Fulbright, M. S. 1995, ApJ, 441, 424
Massey, P., Strobel, K., Barnes, J. V., & Anderson, E. 1988, ApJ, 328, 315
Monet, D. G. et al. 2003, AJ, 125, 984
Moos, H. W. et al. 2000, ApJ, 538, L1
O'Brien, M. S., Bond, H. E., & Sion, E. M. 2001, ApJ, 563, 971
Orosz, J. A., Wade, R. A., Harlow, J. B., Thorstensen, J. R., Taylor, C. J., & Eracleous, M. 1999, AJ, 117, 1598
Pickles, A. J. 1998, PASP, 110, 863
Schreiber, M. R. & Gänsicke, B. T. 2003, A&A, 406, 305
Shortridge K., et al. 2001, Starlink User Note 86.19
Sing, D. K., Holberg, J. B., Barstow, M. A., Burleigh, M., Good, S., Oswalt, T., Howell, S. & Brinkworth, C. 2002, in Proc. 13th European White Dwarf Workshop, ed. R. Silvotti & D. de Martino (Dordrecht: Kluwer), 349
Sion, E. S. 1999, PASP, 111, 532
Stellingwerf, R. F. 1978, ApJ, 224, 953
Wood, M. A. 1995 in 9th European Conference on White Dwarfs, ed. Koester, D. & Werner, K. (Berlin: Springer), 41

Note added in proof.—C. S. Brinkworth, M. R. Burleigh, G. A. Wynn, & T. R. Marsh (MNRAS, 348, L33 [2004]) have reported a low-amplitude photometric variability for the magnetic white dwarf GD 356, which closely resembles HS 1136+6646 in both period and amplitude. They attribute the photometric variability to a dark spot on the stellar surface.